Macromolecules
ARTICLE

Macromolecules **2010**, *43*, 5121–5127 **5121**
DOI: 10.1021/ma1003776

Phase Behavior of Complementary Multiply Hydrogen Bonded End-Functional Polymer Blends

Kathleen E. Feldman,[†] Matthew J. Kade,[‡] E. W. Meijer,[§] Craig J. Hawker,*[,‡,†] and Edward J. Kramer*[,†,⊥]

[†]*Materials Department, University of California, Santa Barbara, California 93106,* [‡]*Department of Chemistry and Biochemistry, University of California, Santa Barbara, California 93106,* [§]*Laboratory of Macromolecular and Organic Chemistry, Eindhoven University of Technology, Eindhoven, The Netherlands, and* [⊥]*Department of Chemical Engineering, University of California, Santa Barbara, California 93106*

Received February 16, 2010; Revised Manuscript Received April 2, 2010

ABSTRACT: Blends of diamidonaphthyridine (Napy) end-functional poly(*n*-butyl acrylate) (PnBA) and ureidopyrimidinone (UPy) end-functional poly(benzyl methacrylate) (PbnMA) were studied as a function of the component molecular weights to compare with prior theoretical predictions.[1] Macroscopic phase separation was observed to be prevented by the reversible association of end-functional polymers to form supramolecular diblock copolymers, resulting in stabilization of the interface between the polymers. At low molecular weights homogeneous microstructures were observed, in contrast to nonfunctional homopolymer blends of the same molecular lengths, which rapidly phase separate over macroscopic length scales. At higher molecular weights, the blend structure was reminiscent of compatibilized homopolymer blends, with the phase-separated domain size rapidly increasing with temperature. To compare with theoretical phase diagrams, the temperature-dependent Flory−Huggins χ parameter was measured, and it was found that PnBA/PbnMA covalent diblock copolymers show unusual lower critical ordering (LCOT) behavior with χ slightly increasing with temperature ($\chi(T) = 0.036 - 0.56/T$).

Introduction

Since the advent of living polymerization and with it the ability to synthesize well-defined block copolymers, much work has been dedicated to understanding and predicting the nanoscale structures that they can form. Because of the immiscibility of most polymer−polymer pairs and the connectivity of block copolymers, phase separation is limited to length scales comparable to chain dimensions, i.e., tens to hundreds of nanometers. The specific microphase structure that is formed is determined primarily by the relative volume fractions of the component blocks,[2−7] although complex architectures such as stars and graft copolymers or polydispersity in the block lengths can shift the phase boundaries somewhat in composition from the simple case of a linear diblock copolymer.[8−13] Additionally, the phase behavior can be altered by swelling with solvent or homopolymer,[14−16] or two polymers with different composition can be blended.[17,18]

In contrast to controlling structure through composition or chain architecture, simple thermal tunability in a polymer structure can be introduced through reversible supramolecular interactions.[19] The nature of the interaction varies widely and most commonly consists of either metal−ligand,[20,21] ionic,[22,23] or hydrogen bonding.[24,25] Incorporation of these into various macromolecular architectures such as diblock,[26−35] triblock,[36−38] multiblock,[39−41] star[42] and graft copolymers,[43−45] blends,[35,46] and gels[47,48] has resulted in remarkably simple thermal control over the polymer structure and related properties.

Theory has also predicted interesting behavior in supramolecular polymer systems;[1,49−51] in particular, regions of macrophase separation, microphase separation, and disordered (miscible) phases are commonly observed. For supramolecular diblock copolymers,[1] several reentrant phase transitions are predicted at molecular weights where the binding energy between the hydrogen bonding end groups on immiscible homopolymers is nearly balanced with χN, where χ is the Flory−Huggins interaction parameter and N is the degree of polymerization. By changing one of the components from a mono-end-functional chain to a telechelic chain, a remarkably rich phase space is predicted,[49] with regions of lamellar, hexagonal, inverted hexagonal, 2-phase, and disorder predicted depending on the blend composition, binding energy, molecular weight, and temperature.

In order to better understand the complicated interplay between polymer assembly and supramolecular interactions, this work presents a simple model system to compare experimentally observed phase behavior with theoretical predictions. The supramolecular diblock architecture was chosen due to the ease with which the chain end-functionalized linear homopolymers could be synthesized, with the well-studied quadruple hydrogen bonded dimer of 2-ureido-4[1*H*]-pyrimidinone (UPy) and 2,7-diamido-1,8-naphthyridine (Napy)[40,52−57] serving as the reversible link between them.

Experimental Section

General Methods. All synthetic procedures were performed under an inert atmosphere of dry nitrogen unless stated otherwise. Solution ^{1}H NMR (500 MHz) and ^{13}C NMR (125 MHz) were performed on a Bruker AVANCE500 spectrometer at room temperature. Proton chemical shifts are reported in ppm downfield from tetramethylsilane (TMS). The following splitting patterns are designated as s, singlet; d, doublet; t, triplet; q, quartet; b, broad; m, multiplet; and dd, double doublet. Carbon chemical shifts are reported downfield from TMS using the resonance of the deuterated solvent as the internal standard.

*To whom correspondence should be addressed. E-mail: hawker@mrl.ucsb.edu (C.J.H.); edkramer@mrl.ucsb.edu (E.J.K.).

Published on Web 05/07/2010

Size exclusion chromatography was carried out at room temperature on a Waters chromatograph connected to a Waters 410 differential refractometer and six Waters Styragel columns (five HR-5 μm and one HWM-20 μm) using THF as eluent (flow rate: 1 mL/min). A Waters 410 differential refractometer and 996 photodiode array detector were employed. The molecular weights of the polymers were calculated relative to linear polystyrene standards.

Differential scanning calorimetry data were acquired on a TA Instruments Q2000 modulated DSC at a heating rate of 5 °C/min. Data presented are from the second heating after a single cycle from −75 to 120 °C. Transmission electron micrographs were acquired on a FEI Tecnai G2 Sphera microscope operating at an accelerating voltage of 200 kV. Optical micrographs were acquired on a Nikon Optiphot-100S microscope. Variable temperature small-angle X-ray scattering (SAXS) was done using an Instec HCS302 heating stage fitted in the beamline of a home-built spectrometer consisting of a fine focus Rigaku rotating anode generator and Bruker HI-STAR multiwire area detector. Samples were allowed to equilibrate at each temperature for 30 min before data acquisition began.

Materials. Methyl 2-phenyl-2-(phenylcarbonothioylthio)-acetate (**1**) was synthesized according to Barner-Kowollik et al.[58] Tetrahydrofuran was dried using a Pure Solv-MD solvent purification system from Advanced Technology. *n*-Butyl acrylate (nBA) and benzyl methacrylate (bnMA) were purified by passing over neutral alumina. Azobis(isobutyronitrile) (AIBN) was recrystallized from methanol. All other chemicals were obtained from Aldrich and used as received.

Supramolecular diblock copolymers consisted of blends of Napy-end-functional poly(*n*-butyl acrylate) (PnBA-Napy) and UPy-end-functional poly(benzyl methacrylate) (PbnMA-UPy) synthesized as previously reported.[59]

P(nBA-*b*-bnMA) covalent diblocks were synthesized via either click coupling as described previously[59] or by reversible addition−fragmentation chain transfer (RAFT) polymerization. In the latter, benzyl methacrylate was polymerized first by the following procedure. Benzyl methacrylate, RAFT agent **1**, and AIBN (0.1 equiv relative to **1**) were dissolved in dioxane at a monomer concentration of 3.3 M. The solution was degassed through three freeze−pump−thaw cycles, sealed in an ampule, and then placed in a 70 °C oil bath for 6 h. The resulting polymer was purified by precipitation into methanol and characterized by GPC. The second block of PnBA was grown by dissolving PbnMA macro-chain-transfer agent in *n*-butyl acrylate monomer with 0.1 equiv of AIBN relative to the RAFT chain end. The mixture was degassed through three freeze−pump−thaw cycles, sealed in an ampule, and then placed in a 70 °C oil bath for 1 h. The diblock was purified by precipitating into methanol. The RAFT chain end was removed according to the procedure of Perrier et al.[60] by reaction with a 100-fold excess of AIBN in dioxane at 80 °C, followed by characterization by GPC and ^{1}H NMR.

Sample Preparation. Solutions for spin-casting consisted of 3 wt % total polymer in toluene with a 1:1 molar ratio of end groups (no excess UPy- or Napy-functional polymer). Films ~100 nm thick for TEM were spun on salt (NaCl) crystals. All samples were annealed under nitrogen for 4 days unless otherwise noted. TEM samples were stained with RuO_4 (which selectively stains PbnMA) for 15 min and floated onto copper grids for imaging.

Samples for SAXS experiments consisted of a small amount of polymer melt packed into the center of a copper washer. Kapton film was epoxied to both sides to seal and contain the sample.

SAXS Data Analysis. SAXS scattering curves in the disordered state for samples P(bnMA$_{112}$-*b*-nBA$_{108}$) and P(bnMA$_{62}$-*b*-nBA$_{77}$) were analyzed using the following equations according to Leibler[2] and Hashimoto[61,62] to give $\chi(T)$. Misprints in eqs 3 and 6 from a previous publication[62] have been corrected.

$$I(q) = \frac{K}{S(q)/W(q) - 2\chi N} \tag{1}$$

$$S(q) = \langle S_{nBA,nBA}(q)\rangle_v + 2\langle S_{nBA,bnMA}(q)\rangle_v + \langle S_{bnMA,bnMA}(q)\rangle_v \tag{2}$$

$$W(q) = \langle S_{nBA,nBA}(q)\rangle_v\langle S_{bnMA,bnMA}(q)\rangle_v - \langle S_{nBA,bnMA}(q)\rangle_v^2 \tag{3}$$

$$\langle S_{X,X}(q)\rangle_v = r_{c,n} f_{X,n}{}^2 g^{(2)}_{X,n}(q) \tag{4}$$

$$\langle S_{nBA,bnMA}(q)\rangle_v = r_{c,n} f_{nBA} f_{bnMA} g^{(1)}_{nBA,n}(q) g^{(1)}_{bnMA,n}(q) \tag{5}$$

$$r_{c,n} = (v_{nBA}N_{nBA,n} + v_{bnMA}N_{bnMA,n})/(v_{nBA}v_{bnMA})^{1/2} \tag{6}$$

$$g^{(1)}_{X,n}(q) = \frac{1}{x_{X,n}}\{1 - [x_{X,n}(\lambda_X - 1) + 1]^{-(\lambda_X - 1)^{-1}}\} \tag{7}$$

$$g^{(2)}_{X,n}(q) = \frac{2}{x_{X,n}{}^2}\{-1 + x_{X,n} + [x_{X,n}(\lambda_X - 1) + 1]^{-(\lambda_X - 1)^{-1}}\} \tag{8}$$

$$x_{X,n} \equiv (N_{X,n}b_X{}^2/6)q^2 \tag{9}$$

$$\lambda_{X,n} = N_{X,w}/N_{X,n} \tag{10}$$

X refers to either PnBA or PbnMA. The average statistical segment length b was used as a fitting parameter to match the peak position and was calculated to be ~0.85 nm, and the molecular volumes were $v_{PbnMA} \sim 149$ cm^3/mol and $v_{PnBA} \sim 116$ cm^3/mol. Because the polymers were synthesized in a stepwise fashion with the PbnMA block first, $\lambda_{PbnMA,n}$ was directly measured as the polymer polydispersity index (PDI). $\lambda_{PnBA,n}$ was then calculated from $\lambda_{diblock,n}$ as

$$\lambda_{PnBA,n} = \frac{\lambda_{diblock,n} - w_{PbnMA}{}^2(\lambda_{PbnMA,n} - 1) - 1}{w_{PnBA}{}^2} + 1 \tag{11}$$

where w_{PbnMA} is the weight fraction of the PbnMA block.

By varying χ (eq 1), the best fits to the data at each temperature in the disordered state were obtained.

Results and Discussion

Having chosen a model polymer system for studying supramolecular diblock copolymers, the behavior of symmetric covalent diblock copolymers was first characterized by variable temperature SAXS to obtain $\chi(T)$. From there, a series of UPy- and Napy-end-functional polymers of increasing molecular weight was synthesized, and their blend morphology was characterized as a function of temperature. By knowing $\chi(T)$ and estimating the binding constant h, the blends can be compared with theoretical predictions.

Estimation of $\chi(T)$ between PnBA and PbnMA. The chosen polymer system consists of poly(*n*-butyl acrylate) (PnBA) and poly(benzyl methacrylate) (PbnMA), which from an estimate of χ based on group contribution calculations were expected to phase separate at moderate molecular weights. Both have relatively low T_gs, providing a wide temperature window for experiments, and PbnMA can be stained by ruthenium tetroxide for TEM characterization. Comparison of multiple hydrogen bonded (MHB) blends with the theoretical phase diagram[1] requires knowledge of the magnitude and temperature dependence of the Flory−Huggins interaction parameter $\chi(T)$ for PnBA and PbnMA, which is often measured through temperature-dependent scattering experiments. The order−disorder transition temperature T_{ODT}s of

a series of symmetric diblocks (see Scheme 1) with increasing total molecular weight can be measured by SAXS, giving values for χ at several temperatures, or scattering curves can be collected at various temperatures in the disordered state and the curves fit to well-known functions related to molecular parameters and χ.

Table 1 lists the covalent diblock copolymers that were synthesized in order to determine $\chi(T)$ for the PnBA/PbnMA system. From initial DSC characterization shown in Figure 1 it appeared that diblock copolymers with a total molecular weight of 33.8K and above were ordered as evidenced by two T_gs near −50 °C (PnBA) and 55 °C (PbnMA). Lower molecular weight diblocks, on the other hand, show no significant transitions between −75 and +100 °C, suggesting that they are disordered.

To confirm the phase behavior, variable temperature SAXS experiments were conducted between 80 and 240 °C, beginning with P(bnMA$_{112}$-*b*-nBA$_{108}$). As the lowest molecular weight ordered diblock, it was expected to have the lowest T_{ODT}. Data are shown in Figure 2, and quite unusual behavior is apparent—a weak second-order scattering peak at $q = 2q^*$ is present at all temperatures above 120 °C (not shown in the figure), and the primary peak is relatively sharp, reflecting a lamellar microphase-separated structure with a periodicity of 25.4 nm. In contrast, at 100 °C and below no second-order peak is present, and the primary peak broadens and decreases in intensity with decreasing temperature. These data are summarized in Figure 2; it is clear that this material *orders* on heating, and thus it has a lower critical ordering transition (LCOT). Although there is some hysteresis (the lamellar order-to-disorder transition is first order as shown by Fredrickson and Helfand,[3] so there is an energy barrier to nucleation), the transition is estimated to occur at 110 °C.

Scheme 1. Structure of Covalent (top) and Supramolecular (bottom) Diblock Copolymers

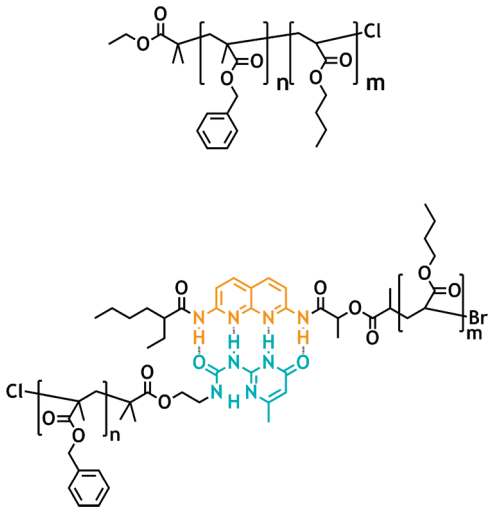

A second diblock copolymer, P(bnMA$_{62}$-*b*-nBA$_{77}$), was characterized by VT SAXS in an attempt to measure $\chi(T)$; because of its lower molecular weight, the LCOT temperature is pushed higher, giving a wider experimentally accessible temperature range in the disordered state. Figure 3 shows the scattering data from 80 to 240 °C, and it is immediately clear that the primary scattering peak is very weak (on the order of 10 times weaker than P(bnMA$_{112}$-*b*-nBA$_{108}$)), and no higher-order peaks are present, confirming that this material is disordered over the entire measured temperature range.

According to Leibler,[2] the scattered intensity in the disordered phase is given by the following equation:

$$I(q) = \frac{K}{S(q)/W(q) - 2\chi N} \tag{12}$$

where K is a constant and equations for $S(q)$ and $W(q)$ are given in the Experimental Section. By fitting the scattering peak in the disordered phase, χ was obtained over a range of temperatures for the two diblocks. Only the lowest temperature data (in the disordered state below 110 °C) were fit for P(bnMA$_{112}$-*b*-nBA$_{108}$). Figure 4 shows $\chi(T)$; although the absolute magnitude of χ varies slightly between the two samples, probably reflecting the uncertainty in the measured molecular weights, in both cases it increases very weakly with temperature.

Typically, χ has the following empirical form in which A is related to entropic effects and B to enthalpic:

$$\chi(T) = A + \frac{B}{T} \tag{13}$$

Fits to this equation for the range over which the data are linear are shown in Figure 4 (for diblock P(bnMA$_{62}$-*b*-nBA$_{77}$) the intensity of the lowest temperature scattering peaks is very low, leading to possible large errors in the measurement of χ). In each case the weak temperature

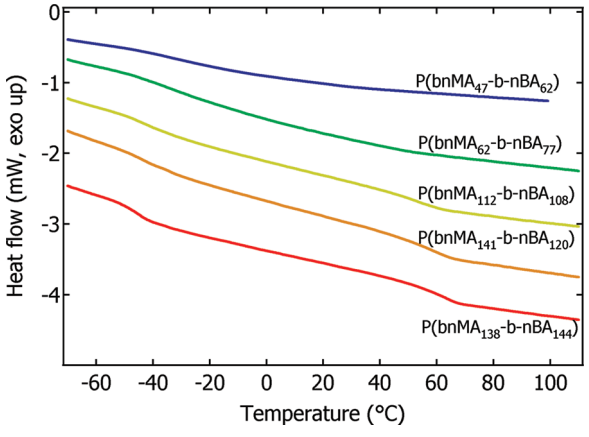

Figure 1. DSC traces (second heating) of covalent diblock copolymers.

Table 1. PbnMA-*b*-PnBA Covalent Diblock Copolymers[a]

	block 1 (PbnMA)			diblock			
sample	M_n	PDI$_{PbnMA}$	$N_{bnMA,n}$	M_n	PDI$_{diblock}$	$N_{nBA,n}$	mol % nBA (^{1}H NMR)
P(bnMA$_{47}$-*b*-nBA$_{62}$)	8 500	1.17	47	16 600	1.27	62	57
P(bnMA$_{62}$-*b*-nBA$_{77}$)	11 200	1.17	62	21 200	1.26	77	55
P(bnMA$_{112}$-*b*-nBA$_{108}$)	20 000	1.31	112	33 800	1.19	108	49
P(bnMA$_{141}$-*b*-nBA$_{120}$)	25 100	1.28	141	40 500	1.16	120	46
P(bnMA$_{138}$-*b*-nBA$_{144}$)	24 600	1.29	138	43 100	1.20	144	51

[a] Subscripts refer to the degree of polymerization of each block. a: PS equivalent, THF GPC.

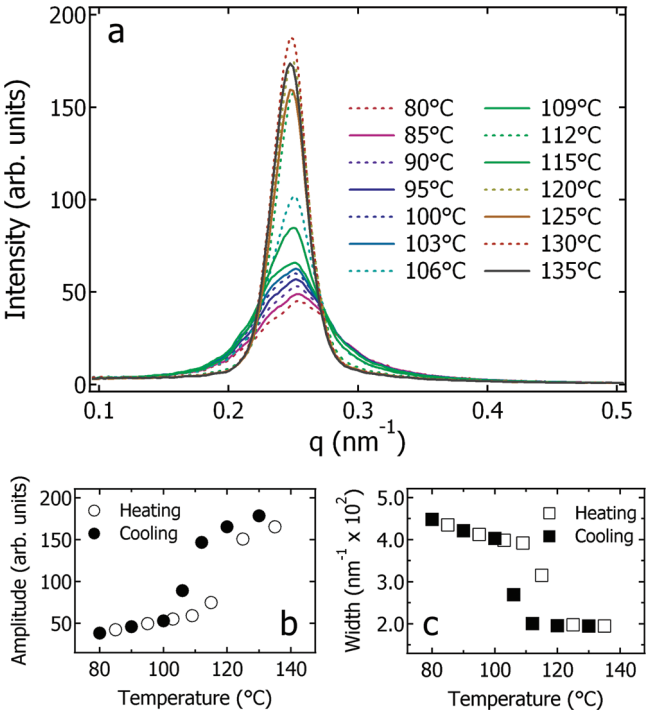

Figure 2. Variable temperature SAXS of P(bnMA$_{112}$-*b*-nBA$_{108}$) (a: primary scattering peak; solid lines, heating; dotted lines, cooling; b: peak amplitude as a function of temperature; c: peak width as a function of temperature).

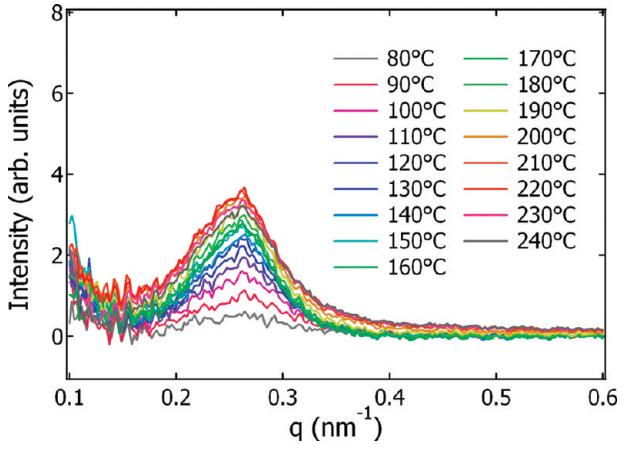

Figure 3. Variable temperature SAXS of P(bnMA$_{62}$-*b*-nBA$_{77}$) (disordered at all measured temperatures).

dependence of χ reflects an extremely small enthalpic contribution ($B = -0.64$ to -0.56); as a reference, $\chi_{PS/PMMA} = 0.0282 + 4.46/T$ and this system is generally considered have a very weak temperature dependence,[62] whereas $\chi_{PS/P2VP} = -0.033 + 63/T$ and this system is considered to be strongly temperature dependent.[63]

Such LCOT behavior is quite uncommon in polymer blends; the system that has been most widely characterized and shows similar behavior is poly(styrene)/poly(butyl methacrylate).[64−66] This behavior has been suggested to depend on a weak overall immiscibility and originate from a positive volume change on demixing (ordering) of the two block segments, increasing the number of available configurations and therefore the entropy of the system.[64] Considering the structural similarity between PS/PnBMA and PbnMA/PnBA, it is perhaps not surprising that the latter should also show LCOT-type behavior. Nevertheless, this

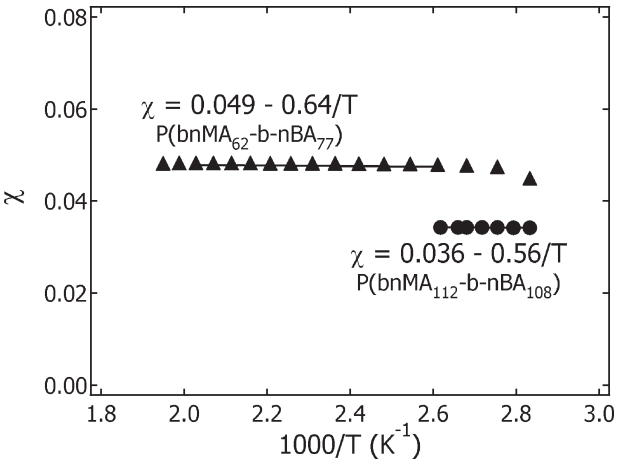

Figure 4. Temperature dependence of the Flory−Huggins χ parameter for PnBA/PbnMA as measured from fits to the disordered phase scattering peaks of symmetric covalent diblock copolymers. Temperature is given in kelvin.

does provide another polymer system with LCOT phase behavior that can be easily synthesized via controlled free radical polymerization and may prove useful as a baroplastic.[67]

Thin Film Microstructure of UPy/Napy-Based Blends. To compare with the theoretical phase diagram,[1] a series of UPy- and Napy-end-functional polymers (see Scheme 1) were synthesized as described previously.[59] The molecular weights were matched as closely as possible so that when blended in a 1:1 ratio of end groups the resulting supramolecular diblocks would be symmetric. For the PnBA/PbnMA system studied here, the axes of the theoretical phase diagram[1] must be considered differently than initially presented. In that work, $h/\chi N$ reflected the binding strength normalized by the polymer−polymer interaction strength, and since both h and χ were assumed to have an inverse temperature dependence, $h/\chi N$ was taken to be independent of temperature. Because $\chi_{PnBA/PbnMA}$ is nearly independent of temperature, the abscissa is now the temperature-dependent axis, with $h/\chi N$ decreasing as $1/T$, and the ordinate ($1/\chi N$) is the temperature-independent axis.

In order to investigate the phase behavior of end-functional supramolecular blends, the component polymers were dissolved in toluene and spin-cast into films ~100 nm thick. The thin film geometry was chosen due to the ease of characterization by standard techniques such as TEM, and it has the additional benefit that by spin-coating from a neutral solvent the initial microstructure is as random as possible.

Figure 5 shows the thin film microstructure of symmetric blends (matched molecular weight and stoichiometry) of PbnMA-UPy and PnBA-Napy as observed by TEM. Each film was spin-cast from toluene solution onto NaCl plates and annealed under nitrogen environment for 4 days before staining with RuO_4 and floating onto the TEM grid. The blend compositions are given in Table 2, and the component molecular weights range from ~10 to ~60 kg/mol. χ is calculated as $0.036 - 0.56/T$ based on the data from P(bnMA$_{112}$-*b*-nBA$_{108}$); although the data from P(bnMA$_{62}$-*b*-nBA$_{77}$) span a wider range of temperature, the weak scattering peak leads to higher uncertainty in the absolute magnitude of the measured χ. As a reference, optical micrographs of a low molecular weight nonfunctional blend are also included and show that in the absence of MHB end groups such blends macrophase separate even at low annealing

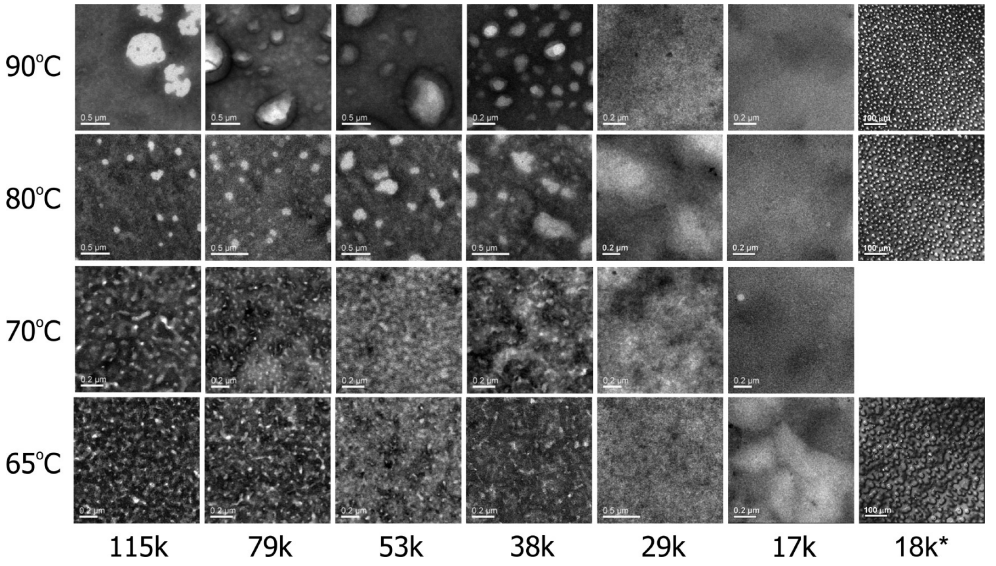

Figure 5. Thin film morphologies of PbnMA-UPy/PnBA-Napy-based blends. Molecular weights are given for the supramolecular diblock (sum of the blend component molecular weights). 18k*: homopolymer blend with no MHB end groups as observed by optical microscopy (note the different scale bars, 0.2 or 0.5 μm vs 100 μm).

Table 2. Supramolecular Blend Compositions[a]

	PbnMA-UPy			PnBA-Napy			supramolecular diblock
blend	M_n (kg/mol)	$N_{bnMA,n}$	PDI	M_n (kg/mol)	$N_{nBA,n}$	PDI	χN (80 °C)
1	9 700	53	1.20	8 000	43	1.14	3.9
2	15 300	85	1.16	14 000	77	1.23	6.6
3	18 900	105	1.14	18 600	103	1.15	8.2
4	29 100	163	1.22	23 700	132	1.14	12.0
5	41 700	235	1.12	37 100	208	1.15	17.2
6	58 200	329	1.12	56 900	321	1.14	25.1
7[b]	8 200	45	1.15	9 900	55	1.10	3.9

[a] χ calculated as $0.036 - 0.56/T$, and $N = N_{A,w} + N_{B,w}$. [b] Homopolymers with no MHB end groups.

temperatures. The experimental phase diagram is arranged to match the theoretical, with molecular weight decreasing from left to right (because the MHB groups are always UPy and Napy, the binding strength h is constant at any given temperature and $h/\chi N$ increases with decreasing N). The lowest molecular weight MHB blends show no structure at any of the temperatures measured, and on increasing the molecular weight above a critical value phase-separated structures are observed, with the average domain size increasing slightly with M_n. With increasing temperature the domain size in the phase-separated blends increases dramatically, although comparison with the nonfunctional blend shows that none are yet fully macrophase-separated. The presence of MHB groups at polymer chain ends has been shown to increase the glass transition temperature,[68] and thus to a value that is possibly above the annealing temperature, resulting in kinetically frozen structures. To confirm that all annealing temperatures were above both polymer T_gs, blends 2 and 3 were measured by DSC between 0 and 100 °C (data not shown). A PbnMA T_g was observed at 55 °C, demonstrating that the chain-end effects on the glass transitions in the blends considered here are minimal. While it is assumed that the observed structures are not fully equilibrated, it has also been shown that even very small concentrations of interfacial diblock copolymer dramatically slow domain coarsening in polymer blends.[69]

Under no conditions were structures observed that resembled traditional covalent diblock copolymers, suggesting that the fraction of supramolecular diblocks is relatively low as demonstrated previously.[59] It is conceivable that these blends are near enough to the Lifshitz points predicted by theory for fluctuations to disrupt any ordered microstructure and generate a bicontinuous microemulsion as previously observed in blends of diblock copolymers and their corresponding homopolymer components.[70] Scattering experiments, either at grazing incidence (GISAXS) for thin films or in transmission for bulk blends, would be required to conclusively identify the structure since the scattering of bicontinuous microemulsions is known to follow the Teubner−Strey dependence on the scattering vector q.[70−72] Bulk SAXS experiments were attempted for blends 1 and 2. To form the blends, the components were dissolved in toluene as for spin-coating and concentrated by evaporation. The resulting mixtures appeared optically opaque, suggesting macrophase separation, and indeed no scattering peaks were observed by SAXS. It is likely that as the solution is being concentrated, the UPy−Napy bond is dynamic enough to allow supramolecular diblocks to break and large-scale phase separation to take place. When spin-coating, however, the solvent is removed much more quickly and the bonds remain intact.

We can infer from the observed morphologies that the driving force for phase separation is generally stronger than that for the formation of supramolecular diblocks. Direct measurement of the equilibrium constant K_a(UPy−Napy) in the melt by common techniques such as variable temperature FTIR or solid-state ^{1}H NMR is complicated by the high binding constant, resulting in extremely low concentrations of unbound UPy and Napy.[73] By comparing the microstructures from Figure 5 with the universal theoretical phase diagram[1] using the values of χN in Table 2, however, the binding free energy h which is normalized by kT is estimated

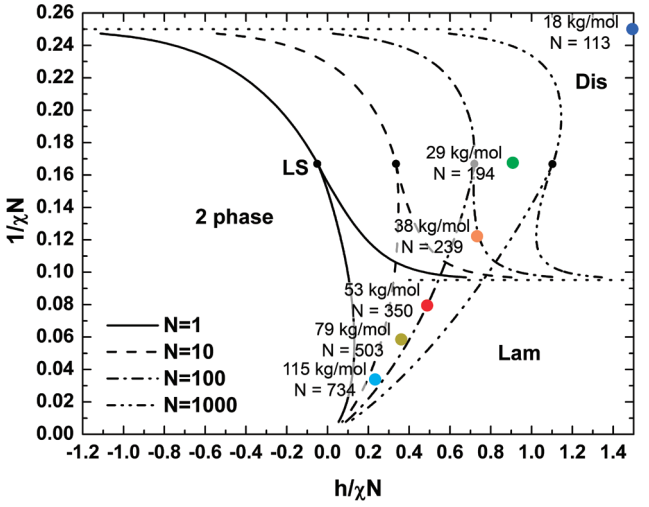

Figure 6. Approximate placement of the supramolecular blends on the theoretical phase diagram corresponding to a temperature of 80 °C. Reproduced with permission from ref 1.

to fall between 5.8 and 6.5 at 80 °C. The resulting placement of the blends on the theoretical phase diagram is shown in Figure 6. By assuming that the free energy change on binding is purely enthalpic, it is then also possible to estimate a UPy−Napy association constant K_a at 30 °C of ∼500−1800 M^{-1}. Interestingly, this estimate is very similar to K_a previously measured in $CHCl_3$ solution for PnBA-tethered UPy and Napy (1200 M^{-1})[74] despite the different "solvent" (PnBA). In that case it was found that a longer alkyl spacer between the MHB group and the polymer backbone recovered the strong binding observed in small molecules, as seen in other related systems.[75,76] From Figure 6 it is clear that in order to access the microphase-separated region of the phase diagram, stronger binding, i.e. larger h, is necessary.

This polymer system was designed assuming that both the binding strength and incompatibility would decrease with temperature, potentially giving interesting phases at temperatures at which the two energies are comparable. With PnBA/PbnMA, however, the MHB blends are driven to phase separate at elevated temperatures both because of a decrease in concentration of supramolecular diblock (the supramolecular diblock copolymer at the interface would reduce interfacial tension and prevent domain coarsening) and because the polymer−polymer compatibility decreases with increasing χ. In terms of the theoretical phase diagram, with an increase in temperature h decreases and χ increases (slightly), leading to a horizontal shift toward the two-phase region with little vertical shift. It should also be noted that the experimental system considered here allows for both UPy−Napy (A−B) and UPy−UPy (A−A) binding, so comparison with the theoretical phase diagram may not be wholly appropriate. It has been shown that at solution concentrations above 0.1 M the UPy−Napy heterodimer is favored by a factor of 20:1,[52] while end-group concentrations in the blends considered here range from approximately 0.1 to 0.01 M. With such a decrease in concentration and lower binding constant than small molecule analogues, it is likely that the selectivity of the UPy−Napy dimerization is compromised and that exclusively heterodimerizing pairs such as UG[77] or deUG[78,79] with Napy might be preferred in future model experiments.

Conclusions

The phase behavior of strongly hydrogen bonded, end-functional polymer blends has been studied as a function of polymer molecular weight and temperature with the significant influence of chain-end functionality being demonstrated.[80,81] All blends consisted of PnBA−Napy and PbnMA−UPy synthesized from functional initiators via ATRP. Disordered structures were found in thin films (∼100 nm) which resembled compatibilized homopolymer blends with structures varying between 20 nm and 1 μm depending on temperature. The lack of ordered lamellar diblock copolymer structures and the very narrow temperature range over which the domains showed significant coarsening indicated that the effects of polymer incompatibility dominated over the stabilization that would be afforded by binding to form supramolecular diblocks. It was found that the PbnMA and PnBA blend system displays an unexpected lower critical ordering transition, with a temperature-dependent Flory−Huggins parameter $\chi(T)$ estimated to be $0.036 - 0.56/T$ (from P($bnMA_{112}$-b-nBA_{108})). With an increase in temperature the blend microstructures coarsened significantly due to two factors—in addition to breaking some fraction of any supramolecular diblock that had formed and thus decreasing the degree of interfacial stabilization, the incompatibility between the phases increased with temperature. Thus, the system was in all ways driven toward macroscopic phase separation, and the temperature window over which diblock copolymer-like structures could be seen was either narrowed or pushed below the T_g of PbnMA.

Acknowledgment. This work was supported by the MRSEC Program of the National Science Foundation under Award DMR05-20415. K.E.F. acknowledges support from NDSEG, NSF, and CSP Technologies fellowships. M.J.K. acknowledges support from an Air Products fellowship.

References and Notes

(1) Feng, E. H.; Lee, W. B.; Fredrickson, G. H. *Macromolecules* **2007**, *40*, 693–702.
(2) Leibler, L. *Macromolecules* **1980**, *13*, 1602–1617.
(3) Fredrickson, G. H.; Helfand, E. *J. Chem. Phys.* **1987**, *87*, 697–705.
(4) Bates, F. S.; Rosedale, J. H.; Fredrickson, G. H. *J. Chem. Phys.* **1990**, *92*, 6255–6270.
(5) Khandpur, A. K.; Forster, S.; Bates, F. S.; Hamley, I. W.; Ryan, A. J.; Bras, W.; Almdal, K.; Mortensen, K. *Macromolecules* **1995**, *28*, 8796–8806.
(6) Matsen, M. W.; Bates, F. S. *Macromolecules* **1996**, *29*, 1091–1098.
(7) Schulz, M. F.; Khandpur, A. K.; Bates, F. S.; Almdal, K.; Mortensen, K.; Hajduk, D. A.; Gruner, S. M. *Macromolecules* **1996**, *29*, 2857–2867.
(8) Grason, G. M. *Phys. Rep.* **2006**, *433*, 1–64.
(9) Smart, T.; Lomas, H.; Massignani, M.; Flores-Merino, M. V.; Perez, L. R.; Battaglia, G. *Nano Today* **2008**, *3*, 38–46.
(10) Lynd, N. A.; Hillmyer, M. A.; Matsen, M. W. *Macromolecules* **2008**, *41*, 4531–4533.
(11) Bang, J.; Kim, S.; Drockenmuller, E.; Misner, M.; Russell, T. P.; Hawker, C. J. *J. Am. Chem. Soc.* **2006**, *128*, 7622–7629.
(12) Lynd, N. A.; Hillmyer, M. A. *Macromolecules* **2005**, *38*, 8803–8810.
(13) Matsen, M. W.; Schick, M. *Macromolecules* **1994**, *27*, 6761–6767.
(14) Vaidya, N. Y.; Han, C. D. *Polymer* **2002**, *43*, 3047–3059.
(15) Han, C. D.; Baek, D. M.; Kim, J.; Kimishma, K.; Hashimoto, T. *Macromolecules* **1992**, *25*, 3052–3067.
(16) Kimishima, K.; Hashimoto, T.; Han, C. *Macromolecules* **1995**, *28*, 3842–3853.
(17) Yamaguchi, D.; Hashimoto, T.; Han, C. D.; Baek, D. M.; Kim, J. K.; Shi, A. C. *Macromolecules* **1997**, *30*, 5832–5842.
(18) Krishnamoorti, R.; Modi, M. A.; Tse, M. F.; Wang, H. C. *Macromolecules* **2000**, *33*, 3810–3817.
(19) de Greef, T. F. A.; Smulders, M. M. J.; Wolffs, M.; Schenning, A. P. H. J.; Sijbesma, R. P.; Meijer, E. W. *Chem. Rev.* **2009**, *109*, 5687–5754.
(20) Kurth, D. G. *Sci. Technol. Adv. Mater.* **2008**, *9*, 014103.
(21) Friese, V. A.; Kurth, D. G. *Coord. Chem. Rev.* **2008**, *252*, 199–211.
(22) Ikkala, O.; ten Brinke, G. *Chem. Commun.* **2004**, 2131–2137.
(23) Hoogenboom, R.; Fournier, D.; Schubert, U. S. *Chem. Commun.* **2008**, 155–162.

(24) Binder, W. H.; Zirbs, R. *Adv. Polym. Sci.* **2007**, *207*, 1−78.
(25) Tang, C.; Lennon, E. M.; Fredrickson, G. H.; Kramer, E. J.; Hawker, C. J. *Science* **2008**, *322*, 429–432.
(26) Yang, X.; Hua, F.; Yamato, K.; Ruckenstein, E.; Gong, B.; Kim, W.; Ryu, C. Y. *Angew. Chem., Int. Ed.* **2005**, *44*, 1907–1907.
(27) Noro, A.; Tamura, A.; Wakao, S.; Takano, A.; Matsushita, Y. *Macromolecules* **2008**, *41*, 9277–9283.
(28) Noro, A.; Nagata, Y.; Takano, A.; Matsushita, Y. *Biomacromolecules* **2006**, *7*, 1696–1699.
(29) Noro, A.; Yamagishi, H.; Matsushita, Y. *Macromolecules* **2009**, *42*, 6335–6338.
(30) Celiz, A. D.; Scherman, O. A. *Macromolecules* **2008**, *41*, 4115–4119.
(31) Yamauchi, K.; Lizotte, J. R.; Hercules, D. M.; Vergne, M. J.; Long, T. E. *J. Am. Chem. Soc.* **2002**, *124*, 8599–8604.
(32) Yamauchi, K.; Lizotte, J. R.; Long, T. E. *Macromolecules* **2002**, *35*, 8745–8750.
(33) Mather, B. D.; Lizotte, J. R.; Long, T. E. *Macromolecules* **2004**, *37*, 9331–9337.
(34) Freitas, L. D.; Jacobi, M. M.; Goncalves, G.; Stadler, R. *Macromolecules* **1998**, *31*, 3379–3382.
(35) Wrue, M. H.; McUmber, A. C.; Anthamatten, M. *Macromolecules* **2009**, *42*, 9255–9262.
(36) Huh, J.; Park, H. J.; Kim, K. H.; Park, C.; Jo, W. H. *Adv. Mater.* **2006**, *18*, 624.
(37) Mather, B. D.; Baker, M. B.; Beyer, F. L.; Berg, M. A. G.; Green, M. D.; Long, T. E. *Macromolecules* **2007**, *40*, 6834–6845.
(38) Moughton, A. O.; Stubenrauch, K.; O'Reilly, R. K. *Soft Matter* **2009**, *5*, 2361–2370.
(39) Binder, W. H.; Bernstorff, S.; Kluger, C.; Petraru, L.; Kunz, M. J. *Adv. Mater.* **2005**, *17*, 2824.
(40) Scherman, O. A.; Ligthart, G. B. W. L.; Ohkawa, H.; Sijbesma, R. P.; Meijer, E. W. *Proc. Natl. Acad. Sci. U.S.A.* **2006**, *103*, 11850–11855.
(41) Binder, W. H.; Kunz, M. J.; Ingolic, E. *J. Polym. Sci., Part A: Polym. Chem.* **2004**, *42*, 162–172.
(42) Gibson, H. W.; Farcas, A.; Jones, J. W.; Ge, Z.; Huang, F.; Vergne, M.; Hercules, D. M. *J. Polym. Sci., Part A: Polym. Chem.* **2009**, *47*, 3518–3543.
(43) Ruokolainen, J.; Mäkinen, R.; Torkkeli, M.; Mäkelä, T.; Serimaa, R.; ten Brinke, G.; Ikkala, O. *Science* **1998**, *280*, 557–560.
(44) Ruokolainen, J.; Saariaho, M.; Ikkala, O.; ten Brinke, G.; Thomas, E. L.; Torkkeli, M.; Serimaa, R. *Macromolecules* **1999**, *32*, 1152–1158.
(45) Ohkawa, H.; Ligthart, G. B. W. L.; Sijbesma, R. P.; Meijer, E. W. *Macromolecules* **2007**, *40*, 1453–1459.
(46) Park, T.; Zimmerman, S. C.; Nakashima, S. *J. Am. Chem. Soc.* **2005**, *127*, 6520–6521.
(47) Noro, A.; Matsushita, Y.; Lodge, T. P. *Macromolecules* **2008**, *41*, 5839–5844.
(48) Noro, A.; Matsushita, Y.; Lodge, T. P. *Macromolecules* **2009**, *42*, 5802–5810.
(49) Lee, W. B.; Elliott, R.; Katsov, K.; Fredrickson, G. H. *Macromolecules* **2007**, *40*, 8445–8454.
(50) Huh, J.; ten Brinke, G. *J. Chem. Phys.* **1998**, *109*, 789–797.
(51) Elliott, R.; Fredrickson, G. H. *J. Chem. Phys.* **2009**, *131*, 144906.
(52) Ligthart, G. B.W. L.; Ohkawa, H.; Sijbesma, R. P.; Meijer, E. W. *J. Am. Chem. Soc.* **2005**, *127*, 810–811.
(53) Li, X. Q.; Jiang, X. K.; Wang, X. Z.; Li, Z. T. *Tetrahedron* **2004**, *60*, 2063–2069.
(54) de Greef, T. F. A.; Ligthart, G. B. W. L.; Lutz, M.; Spek, A. L.; Meijer, E. W.; Sijbesma, R. P. *J. Am. Chem. Soc.* **2008**, *130*, 5479–5486.
(55) Zhao, X.; Wang, X. Z.; Jiang, X. K.; Chen, Y. Q.; Li, Z. T.; Chen, G. J. *J. Am. Chem. Soc.* **2003**, *125*, 15128–15139.
(56) Wang, X. Z.; Li, X. Q.; Shao, X. B.; Zhao, X.; Deng, P.; Jiang, X. K.; Li, Z. T.; Chen, Y. Q. *Chem.—Eur. J.* **2003**, *9*, 2904–2913.
(57) Scherman, O. A.; Ligthart, G. B.W. L.; Sijbesma, R. P.; Meijer, E. W. *Angew. Chem., Int. Ed.* **2006**, *45*, 2072–2076.
(58) Barner-Kowollik, C.; Perrier, S. *J. Polym. Sci., Part A: Polym. Chem.* **2008**, *46*, 5715–5723.
(59) Feldman, K. E.; Kade, M. J.; de Greef, T. F. A.; Meijer, E. W.; Kramer, E. J.; Hawker, C. J. *Macromolecules* **2008**, *41*, 4694–4700.
(60) Perrier, S.; Takolpuckdee, P.; Mars, C. A. *Macromolecules* **2005**, *38*, 2033–2036.
(61) Sakurai, S.; Mori, K.; Okawara, A.; Kimishima, K.; Hashimoto, T. *Macromolecules* **1992**, *25*, 2679–2691.
(62) Zhao, Y.; Sivaniah, E.; Hashimoto, T. *Macromolecules* **2008**, *41*, 9948–9951.
(63) Dai, K. H.; Kramer, E. J. *Polymer* **1994**, *35*, 157–161.
(64) Ruzette, A. V. G.; Banerjee, P.; Mayes, A. M.; Pollard, M.; Russell, T. P.; Jerome, R.; Slawecki, T.; Hjelm, R.; Thiyagarajan, P. *Macromolecules* **1998**, *31*, 8509–8516.
(65) Ruzette, A. V. G.; Mayes, A. M.; Pollard, M.; Russell, T. P.; Hammouda, B. *Macromolecules* **2003**, *36*, 3351–3356.
(66) Russell, T. P.; Karis, T. E.; Gallot, Y.; Mayes, A. M. *Nature* **1994**, *368*, 729–731.
(67) Gonzalez-Leon, J. A.; Acar, M. H.; Ryu, S. W.; Ruzette, A. V. G.; Mayes, A. M. *Nature* **2003**, *426*, 424–428.
(68) vanBeek, D. J. M.; Spiering, A. J. H.; Peters, G. W. M.; teNijenhuis, K.; Sijbesma, R. P. *Macromolecules* **2007**, *40*, 8464–8475.
(69) Yoon, Y.; Hsu, A.; Leal, L. G. *Phys. Fluids* **2007**, *19*, 023102.
(70) Bates, F. S.; Maurer, W. W.; Lipic, P. M.; Hillmyer, M. A.; Almdal, K.; Mortensen, K.; Fredrickson, G. H.; Lodge, T. P. *Phys. Rev. Lett.* **1997**, *79*, 849–852.
(71) Morkved, T. L.; Stepanek, P.; Krishnan, K.; Bates, F. S.; Lodge, T. P. *J. Chem. Phys.* **2001**, *114*, 7247–7259.
(72) Teubner, M.; Strey, R. *J. Chem. Phys.* **1987**, *87*, 3195–3200.
(73) Feldman, K. E.; Kade, M. J.; Meijer, E. W.; Hawker, C. J.; Kramer, E. J. *Macromolecules* **2009**, *42*, 9072–9081.
(74) de Greef, T. F. A. Ph.D. Thesis, Technische Universiteit Eindhoven, **2008**.
(75) de Greef, T. F. A.; Nieuwenhuizen, M. M. L.; Stals, P. J. M.; Fitie, C. F. C.; Palmans, A. R. A.; Sijbesma, R. P.; Meijer, E. W. *Chem. Commun.* **2008**, 4306–4308.
(76) de Greef, T. F. A.; Nieuwenhuizen, M. M. L.; Sijbesma, R. P.; Meijer, E. W. *J. Org. Chem.* **2010**, *75*, 598–610.
(77) Park, T.; Todd, E. M.; Nakashima, S.; Zimmerman, S. C. *J. Am. Chem. Soc.* **2005**, *127*, 18133–18142.
(78) Ong, H. C.; Zimmerman, S. C. *Org. Lett.* **2006**, *8*, 1589–1592.
(79) Kuykendall, D. W.; Anderson, C. A.; Zimmerman, S. C. *Org. Lett.* **2009**, *11*, 61–64.
(80) Hawker, C. J.; Barclay, G. G.; Dao, J. J. *J. Am. Chem. Soc.* **1996**, *118*, 11467–11471.
(81) Rodlert, M.; Harth, E.; Rees, I.; Hawker, C. J. *J. Polym. Sci., Part A: Polym. Chem.* **2000**, *38*, 4749–4763.